

# The antihelmintic flubendazole inhibits microtubule function through a mechanism distinct from Vinca alkaloids and displays preclinical activity in leukemia and myeloma

Paul A. Spagnuolo,<sup>1</sup> Jiayi Hu,<sup>1</sup> Rose Hurren,<sup>1</sup> Xiaoming Wang,<sup>1</sup> Marcela Gronda,<sup>1</sup> Mahadeo A. Sukhai,<sup>1</sup> Ashley Di Meo,<sup>1</sup> Jonathan Boss,<sup>1</sup> Iman Ashali,<sup>1</sup> Reza Beheshti Zavareh,<sup>1</sup> Noah Fine,<sup>1</sup> Craig D. Simpson,<sup>1</sup> Sumaiya Sharmeen,<sup>1</sup> Rob Rottapel,<sup>1</sup> and Aaron D. Schimmer<sup>1</sup>

<sup>1</sup>Princess Margaret Hospital, Ontario Cancer Institute, Toronto, ON

**On-patent and off-patent drugs with previously unrecognized anticancer activity could be rapidly repurposed for this new indication given their prior toxicity testing. To identify such compounds, we conducted chemical screens and identified the antihelmintic flubendazole. Flubendazole induced cell death in leukemia and myeloma cell lines and primary patient samples at nanomolar concentrations. Moreover, it delayed tumor growth in leu-**

**kemia and myeloma xenografts without evidence of toxicity. Mechanistically, flubendazole inhibited tubulin polymerization by binding tubulin at a site distinct from vinblastine. In addition, cells resistant to vinblastine because of overexpression of P-glycoprotein remained fully sensitive to flubendazole, indicating that flubendazole can overcome some forms of vinblastine resistance. Given the different mechanisms of action, we evaluated**

**the combination of flubendazole and vinblastine in vitro and in vivo. Flubendazole synergized with vinblastine to reduce the viability of OCI-AML2 cells. In addition, combinations of flubendazole with vinblastine or vincristine in a leukemia xenograft model delayed tumor growth more than either drug alone. Therefore, flubendazole is a novel microtubule inhibitor that displays preclinical activity in leukemia and myeloma. (*Blood*. 2010;115(23):4824-4833)**

## Introduction

Drugs approved or tested experimentally for indications other than cancer that possess previously unrecognized cytotoxicity toward malignant cells could be rapidly repurposed for this new indication given their prior toxicity testing in humans and animals. For example, the oral hypoglycemic metformin activates the adenosine monophosphate-activated protein kinase pathway through a mechanism dependent on the tumor suppressor LKB1.<sup>1</sup> At pharmacologically achievable concentrations, metformin inhibited the growth of prostate and colon cancer cells and delayed tumor growth in xenografts.<sup>2</sup> Moreover, patients with diabetes receiving metformin had a reduced risk of pancreatic cancer compared with diabetics not receiving metformin.<sup>3</sup> Given data such as these, metformin is currently being evaluated in clinical trials for the treatment of patients with advanced solid tumors.<sup>4</sup> Likewise, thalidomide was discovered to possess antimyeloma activity<sup>5</sup> and was repurposed for this new indication. The identification of thalidomide and its derivative lenolidamide as anticancer agents improved standard care for patients with this hematologic disease.<sup>6</sup>

To date, the identification of drugs with unanticipated anticancer effects has been largely serendipitous. Here we used a systematic approach to identify compounds with unanticipated anticancer activity by testing an in-house chemical library of on-patent and off-patent drugs for their ability to reduce the growth and viability of leukemia cell lines. From these screens, we identified flubendazole, a member of the benzimidazole family of antihelmintic drugs, with potential antileukemia and antimyeloma

activity. Flubendazole has been extensively evaluated in humans and animals for the treatment of intestinal parasites as well as for the treatment of systemic worm infections. In these studies, patients have received up to 50 mg/kg orally daily for 24 months without serious adverse effects.<sup>7-9</sup> Healthy volunteers have also received single oral doses up to 2000 mg without toxicity.<sup>10</sup> In mice receiving a single dose of 5 mg/kg flubendazole, a maximal concentration ( $C_{max}$ ) of 1.12  $\mu\text{g/mL}$  (3.6  $\mu\text{M}$ ) and an area under the curve (AUC) of 2.17  $\mu\text{g}/\text{hour}$  per milliliter with no evidence of toxicity was recorded.<sup>11</sup>

Although selected members of the benzimidazole family have recently been reported to induce cell death in solid tumor cell lines,<sup>12,13</sup> the antitumor properties of flubendazole have not been previously reported. Moreover, the mechanism by which benzimidazoles exert their effects as antihelmintics and by which they induce cell death in malignant cells is not fully understood and several cellular responses have been described. For example, benzimidazoles have been shown to inhibit amino peptidase activity and glutamate catabolism, reduce glucose uptake, increase intracellular calcium levels, and inhibit microtubule formation.<sup>14-16</sup>

Here we demonstrate that flubendazole displays antileukemia and antimyeloma activity in vitro and in vivo at pharmacologically achievable concentrations. Mechanistically, flubendazole alters tubulin structure and function by interacting with a site on tubulin distinct from Vinca alkaloid microtubule inhibitors.

Submitted September 9, 2009; accepted March 4, 2010. Prepublished online as *Blood* First Edition paper, March 26, 2010; DOI 10.1182/blood-2009-09-243055.

The publication costs of this article were defrayed in part by page charge payment. Therefore, and solely to indicate this fact, this article is hereby marked "advertisement" in accordance with 18 USC section 1734.

The online version of this article contains a data supplement.

© 2010 by The American Society of Hematology

## Methods

### Reagents

Colchicine, taxol, and benzimidazole compounds were purchased from Sigma-Aldrich. Vinblastine was purchased from Calbiochem. Drugs were prepared in dimethyl sulfoxide.

### Cell culture

The culture of cells was carried out as previously described.<sup>17</sup> For a detailed description of cell culture, see the supplemental Methods (available on the *Blood* Web site; see the Supplemental Materials link at the top of the online article).

### Cell growth and viability assays

Cell growth and viability were measured using the 3-(4,5-dimethylthiazol-2-yl)-5-(3-carboxymethoxyphenyl)-2-(4-sulfophenyl)-2H-tetrazolium inner salt (MTS) reduction assay (Promega) according to the manufacturer's protocol and as previously described.<sup>18</sup> Cells were seeded in 96-well plates and treated with drug for 72 hours. Optical density was measured at 490 nm. Cell viability was also assessed by the Trypan blue exclusion assay and by annexin V and propidium iodide (PI) staining (Biovision), as previously described.<sup>17</sup>

Clonogenic growth assays with fresh primary acute myeloid leukemia (AML) patient and normal hematopoietic stem cells were performed as previously described.<sup>17</sup> For a detailed description of the clonogenic growth assays, see the supplemental Methods.

Mitotic catastrophe was measured by enumerating the number of multinucleated cells similar to the method previously described.<sup>19</sup> A more detailed description of the assessment of mitotic catastrophe is presented in the supplemental Methods.

### Analysis of gene expression

Changes in gene expression were measured in U937 leukemia cells treated with 1  $\mu$ M flubendazole or buffer control for 4 hours using Ingenuity Pathways Analysis ([www.ingenuity.com](http://www.ingenuity.com)) and the Database for Annotation, Visualization and Integrated Discovery (<http://david.abcc.ncifcrf.gov>). For a detailed description of gene expression analysis, see the supplemental Methods.

### Leukemia and myeloma xenograft models

Sublethally irradiated SCID mice were injected subcutaneously in the left flank with leukemia OCI-AML2 ( $2.0 \times 10^6$ ) or myeloma OPM2 ( $1.0 \times 10^7$ ) cells. Mice were then randomly assigned to receive flubendazole (in 0.9% NaCl and 0.01% Tween-80) or vehicle control (0.9% NaCl and 0.01% Tween-80) intraperitoneally. When the combination of flubendazole and vinblastine or vincristine was evaluated, mice were randomly assigned to receive flubendazole (in 0.9% NaCl and 0.01% Tween-80), vinblastine (in phosphate-buffered saline and 0.01% Tween-20), or vincristine (in phosphate-buffered saline and 0.01% Tween-20), the combination of flubendazole and vinblastine or vincristine, or vehicle control intraperitoneally. Tumor volumes (tumor length  $\times$  width<sup>2</sup>  $\times$  0.5236) were monitored daily using calipers. During drug treatment, animal body weights were measured and recorded every 2 to 3 days. Changes in mouse behavior, including feeding pattern, posture, and overall activity, were monitored and recorded daily. At the end of the experiment (16-18 days), mice were killed, tumors excised, and tumor volume and weight measured. In addition, at the conclusion of the experiment, a necropsy was performed and the organs were examined for gross morphologic alterations. Animal studies were carried out according to the regulations of the Canadian Council on Animal Care and with the approval of the Princess Margaret Hospital ethics review board.

### Assessment of glucose uptake

The effect of flubendazole on the uptake of 2-deoxy-D-glucose in OCI-AML2 cells was performed using a radioactive glucose uptake assay as described by Wood et al.<sup>20</sup> For a detailed description of the assessment of glucose uptake, see the supplemental Methods.

### Tubulin polymerization assay

Polymerization of bovine tubulin was measured according to Beyer et al.<sup>21</sup> Briefly, bovine tubulin (1.8 mg/mL; Cytoskeleton) was added to ice-cold polymerization buffer (PEM: 80mM PIPES, 0.5mM EGTA, 2mM MgCl<sub>2</sub>, 10% glycerol, and 1mM GTP) and centrifuged at top speed in a microcentrifuge for 5 minutes at 4°C. Supernatant (100  $\mu$ L/well) was immediately added to a 96-well plate, which contained colchicine, taxol, flubendazole, or buffer/dimethyl sulfoxide control in PEM buffer. Final drug concentrations were similar to those previously described.<sup>13</sup> After addition of tubulin, the plate was immediately placed in the spectrophotometer, which was maintained at 37°C, and the absorbance measured every 3 minutes for 2.5 hours at 340 nm.

### Measurement of tubulin sulfhydryl groups

The ability of microtubule target drugs to alter tubulin structure was assessed by measuring the number of reactive cysteine residues using the sulfhydryl reagent 5,5'-dithio-bis(2-nitrobenzoic acid) (DTNB; Sigma-Aldrich) as previously described.<sup>13,22</sup> Bovine tubulin (1.5  $\mu$ M) was incubated with 10  $\mu$ M vinblastine, 100  $\mu$ M flubendazole, or a control for 15 minutes at 4°C. After incubation, DTNB was added (100  $\mu$ M final concentration) and the absorbance was measured in a 1-cm path length cuvette at 412 nm for 60 minutes at 37°C. The number of sulfhydryl groups were determined using a molar extinction coefficient for DTNB of 13 600 M<sup>-1</sup>  $\cdot$  cm<sup>-1</sup>.<sup>22</sup>

### Determining the site of tubulin binding

The site of flubendazole binding was determined similar to Gupta et al.<sup>13</sup> Bovine tubulin (5  $\mu$ M) was incubated with 100  $\mu$ M flubendazole, 100  $\mu$ M vinblastine, or buffer control for 30 minutes at 37°C. Colchicine (10  $\mu$ M) was then added and incubated for an additional 60 minutes at 37°C. Fluorescence of the colchicine-tubulin complex was subsequently measured at excitation and emission wavelengths of 360 nm and 430 nm, respectively.

### Determining the effect of flubendazole on microtubules in cultured cells

The morphology of PPC-1 cells incubated with vehicle control or 1  $\mu$ M flubendazole was examined by confocal microscopy. For a detailed description of confocal microscopy, see the supplemental Methods.

### Cell migration assays

HeLa cell migration was measured as previously described.<sup>23</sup> For a detailed description of cell migration assays, see the supplemental Methods.

### Cell-cycle analysis

Cell-cycle analysis was performed as previously described.<sup>24</sup> For a detailed description of cell-cycle analysis, see the supplemental Methods.

### Assessment of sensory function with the tail-flick assay

Sensory function was assessed with the tail-flick assay by Chempartners Co similar to that previously described.<sup>25</sup> Briefly, 50 experimentally naive, male, adult C57BL/6J mice from Shanghai SLAC Co Ltd were treated with 50, 100, or 200 mg/kg flubendazole in 0.9% NaCl and 0.01% Tween-80 or vehicle control (n = 10 per group). Before and after 14 days of treatment, tail-flick latency was measured by applying a high-intensity, noxious, radiant heat stimulus 20 mm from the tip of the tail. When a withdrawal tail-flick response occurred, the thermal stimulus was terminated automatically and the response latency was measured electronically.

### Drug combination studies

The combination index (CI) was used to evaluate the interaction between flubendazole and other therapeutic agents. OCI-AML2 cells were treated with increasing concentrations of flubendazole, vinblastine, colchicine,

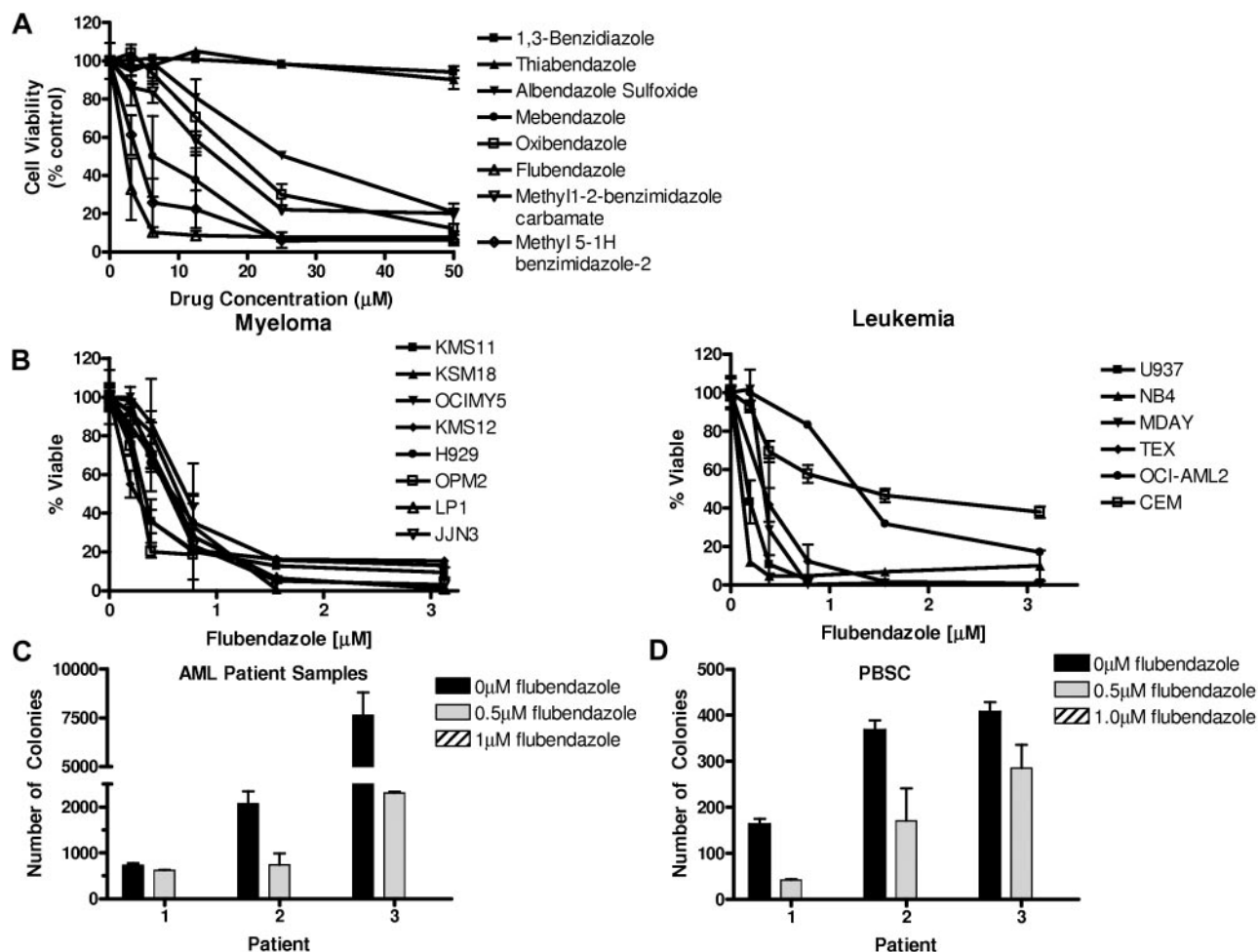


**Figure 1. Flubendazole induces cell death in malignant cell lines.** (A) OCI-AML2 cells were treated for 72 hours with increasing concentrations of benzimidazoles. After incubation, cell growth and viability were measured by the MTS assay. Data are the mean percentage of viable cells  $\pm$  SD from a representative experiment. (B) Leukemia and myeloma cell lines were treated with increasing concentrations of flubendazole. Seventy-two hours after incubation, cell growth and viability were measured by the MTS assay. Data are the mean percentage of viable cells  $\pm$  SD from representative experiments. (C) Primary AML patient samples or (D) primary normal hematopoietic cells ( $1 \times 10^5$  cells;  $n = 3$ ) were plated in a methylcellulose colony-forming assay with increasing concentrations of flubendazole. Colonies were counted 7 days after plating, as described in the supplemental Methods. Data are the mean  $\pm$  SD from 3 independent experiments performed in duplicate.

daunorubicin, or cytarabine. Seventy-two hours after incubation, cell viability was measured by the MTS assay. The Calcsyn median effect model was used to calculate the CI values and evaluate whether the combination of flubendazole with vinblastine, cytarabine, daunorubicin, or colchicine was synergistic, antagonistic, or additive. CI values of less than 1 indicate synergism, CI values equal to 1 indicate additivity, and CI values more than 1 indicate antagonism.<sup>26</sup>

### Statistical analysis

Unless otherwise stated, the results are presented as mean plus or minus SD. Data were analyzed using GraphPad Prism 4.0 (GraphPad Software).  $P$  less than .05 was accepted as being statistically significant. Drug combination data were analyzed using Calcsyn software (Biosoft).

## Results

### A screen of on-patent and off-patent drugs for compounds with novel anticancer activity identifies flubendazole

To identify drugs with unanticipated anticancer activity, we compiled a library of 110 on-patent and off-patent drugs focused on antimicrobials and metabolic regulators with a wide therapeutic index and well-characterized pharmacokinetics that were available

from the Canadian and United States drug formularies. We then screened this library at increasing concentrations, using the MTS assay, to identify compounds that reduced the growth and viability of 3 leukemia cell lines after 72 hours of incubation.<sup>27</sup> From these screens, we identified several cytotoxic agents, including mebendazole. Mebendazole is a member of the benzimidazole family of antihelmintics, so we investigated the cytotoxicity of this drug class. OCI-AML2 leukemia cells were treated with increasing concentrations of 8 benzimidazole family members. Seventy-two hours after incubation, cell growth and viability were measured by the MTS assay. The most potent benzimidazole in this panel was flubendazole (Figure 1A).

### Flubendazole is cytotoxic to leukemia and myeloma cell lines

Having identified flubendazole as a potential anticancer agent, we evaluated its effects in a panel of malignant cell lines. Leukemia and myeloma cell lines were treated with increasing concentrations of flubendazole. Seventy-two hours after incubation, cell growth and viability were measured by the MTS assay. Flubendazole reduced cell viability with an 50% inhibitory concentration (IC<sub>50</sub>) less than 1 μM in 8 of 8 myeloma and 4 of 6 leukemia cell lines, including MDAY-D2 cells with an IC<sub>50</sub> of 3nM (Figure 1B). Of

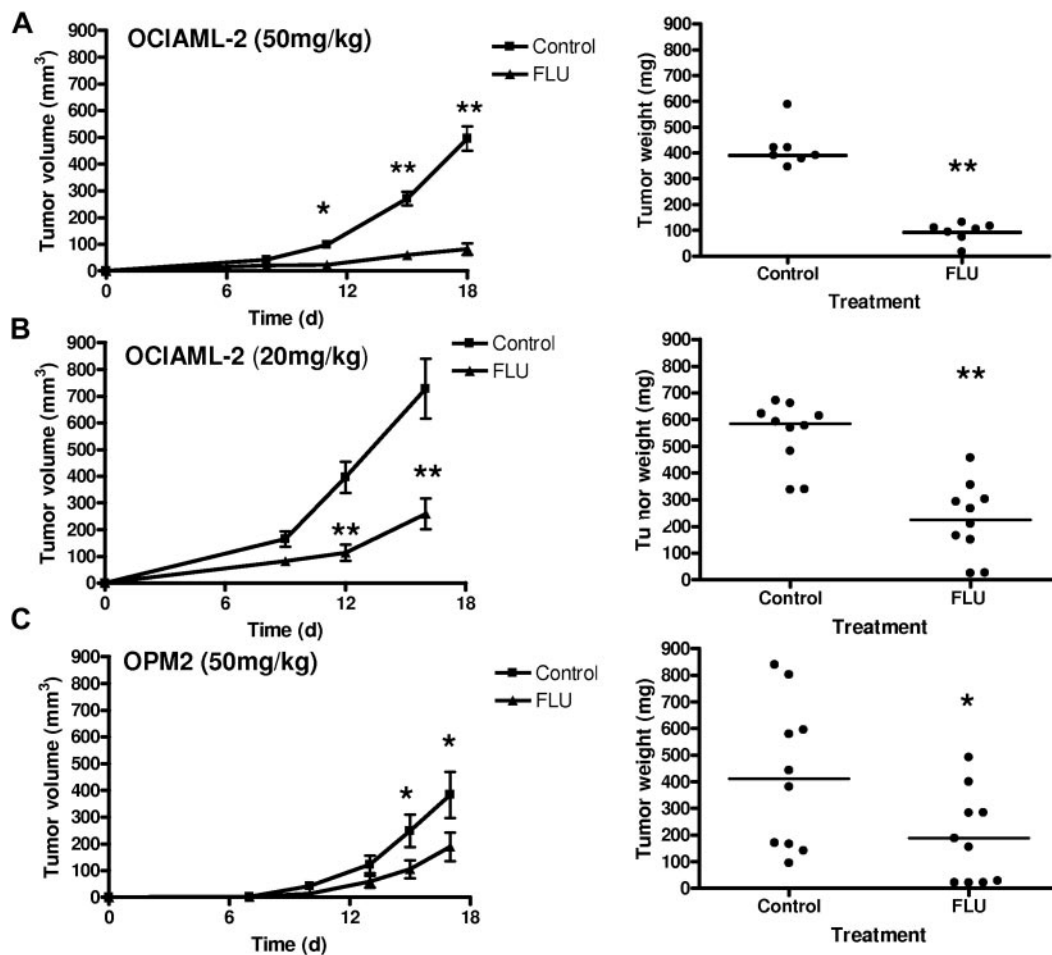


**Figure 2.** Flubendazole delays tumor growth and reduces tumor weight in leukemia and myeloma mouse xenografts. Sublethally irradiated SCID mice were injected subcutaneously with OCI-AML2 cells ( $n = 20$ ; 10 per group). After implantation, mice were treated with 50 mg/kg flubendazole (A), 20 mg/kg flubendazole (B), or vehicle control by intraperitoneal injection daily. Tumor volume was measured over time. After 16 days (20 mg/kg dose) or 18 days (50 mg/kg dose), mice were killed and tumors were excised, measured, and weighed. (C) Sublethally irradiated SCID mice were injected subcutaneously with OPM2 cells ( $n = 20$ ; 10 per group). Mice were treated with 50 mg/kg flubendazole or vehicle control by intraperitoneal injection twice daily. Tumor volume and body weight were measured over time. After 17 days, mice were killed and tumors were excised, measured, and weighed. Data are mean  $\pm$  SEM. Differences in tumor volume and tumor weight were analyzed by an unpaired *t* test \*\* $P < .001$ , \* $P < .05$ .

note, the remaining 2 cell lines (OCI-AML-2 and CEM) had  $IC_{50}$  values of 1.1 plus or minus 0.6 and 1.9 plus or minus 0.9  $\mu$ M, respectively. Concentrations of 1  $\mu$ M appear pharmacologically achievable, based on prior studies in mice that demonstrated a dose of 5 mg/kg produced a  $C_{max}$  of 1.12  $\mu$ g/mL (3.6  $\mu$ M)<sup>11</sup> and an AUC of 2.17  $\mu$ g/hour per milliliter without toxicity.<sup>10</sup> Cell death was confirmed by PI staining and trypan blue exclusion assay (annexin<sup>-</sup>/PI<sup>-</sup>: 0  $\mu$ M, 94.2  $\pm$  1.9; 1.5  $\mu$ M, 59.4  $\pm$  1.0; 2  $\mu$ M, 45.8  $\pm$  1.1; supplemental Figure 1). We also evaluated the effects of flubendazole in primary normal hematopoietic cells obtained from donors of G-CSF-mobilized peripheral blood for allotransplantation (PBSC). In contrast to the effects observed in leukemia cell lines, treatment of PBSCs with 2  $\mu$ M flubendazole for 24 hours induced minimal cell death (annexin<sup>-</sup>/PI<sup>-</sup>: 0  $\mu$ M, 93.0  $\pm$  4.5; 2  $\mu$ M, 89.0  $\pm$  4.9).

Flubendazole was also evaluated in clonogenic growth assays with primary AML and normal hematopoietic samples. Flubendazole reduced the clonogenic growth of primary AML blasts ( $n = 3$ ) from peripheral blood samples obtained from patients with AML (intermediate-risk cytogenetics,  $n = 2$ ; and poor-risk cytogenetics,  $n = 1$ ), and complete loss of clonogenic growth was observed after treatment with 1  $\mu$ M flubendazole (Figure 1C). However, similar reductions in clonogenic growth were also observed when PBSCs were treated with flubendazole with complete loss of clonogenic

growth with 1  $\mu$ M flubendazole (Figure 1D). Thus, flubendazole displays activity against leukemia and myeloma cells at nanomolar concentrations, but there is a narrow difference between primary AML and normal hematopoietic cells in clonogenic growth assays.

#### Flubendazole delays tumor growth in leukemia and myeloma xenografts

As flubendazole was cytotoxic to malignant cells in vitro, we evaluated its antitumor effects in leukemia and myeloma xenografts. OCI-AML2 leukemia cells were injected subcutaneously into sublethally irradiated SCID mice. Mice were then treated daily with flubendazole (20 or 50 mg/kg) or vehicle control intraperitoneally. Compared with mice treated with vehicle control, flubendazole significantly delayed tumor growth and reduced tumor weights ( $P < .001$ ; Figure 2A-B). Likewise, sublethally irradiated SCID mice were injected subcutaneously with OPM2 myeloma cells. Mice were then treated daily with 50 mg/kg flubendazole or buffer control for 17 days intraperitoneally. Flubendazole significantly delayed tumor growth and reduced tumor weights compared with mice treated with vehicle control ( $P < .05$ ; Figure 2C).

In both leukemia and myeloma models, no significant differences in body weight were observed in flubendazole-treated mice

compared with control (supplemental Figure 2). Likewise, flubendazole treatment did not alter the behavior of the mice or produce gross organ changes on necropsy. Thus, flubendazole displays novel preclinical activity against leukemia and myeloma at concentrations that appear pharmacologically achievable.

### Flubendazole does not alter glucose uptake

In studies with the parasite *Trichuris globulosa*, the antihelmintic effects of the benzimidazoles thiabendazole and fenbendazole were related to inhibition of glucose uptake with resultant alterations in glucose metabolism.<sup>15</sup> Therefore, we tested the effects of flubendazole on glucose uptake in malignant cells. OCI-AML2 cells were treated with increasing concentrations of flubendazole for 16 hours, and uptake of <sup>3</sup>H-deoxy-D-glucose was measured (supplemental Figure 3A). In contrast to the observations in the parasite, flubendazole at concentrations up to 4 μM did not alter glucose uptake. Likewise, culturing cells with various concentrations of glucose did not alter flubendazole-induced death (supplemental Figure 3B). Thus, flubendazole-induced cell death does not appear related to inhibition of glucose uptake.

### Flubendazole alters microtubule structure and function

To better understand the mechanism by which flubendazole induced death of malignant cells, we examined changes in gene expression after 4 hours of flubendazole treatment. By gene ontology and pathway analysis, 196 genes were identified to be deregulated more than 4-fold with flubendazole treatment (ArrayExpress accession: E-MEXP-2352; supplemental Table 1). Of these, 179 genes were annotated and 58 of 179 fell within 8 functional annotations associated with chromosomal segregation and cytoskeleton regulation; genes involved in chromosomal segregation were the most affected by flubendazole treatment (supplemental Table 2). Moreover, by connectivity map analysis, changes in gene expression were found to be similar to gene signatures induced by the known tubulin inhibitors nocodazole and colchicine (data not shown).

Given these findings and previous observations that benzimidazoles such as mebendazole exert an antihelmintic effect at least in part by inhibiting tubulin polymerization, we evaluated the effects of flubendazole on tubulin structure and polymerization. To determine whether flubendazole alters tubulin structure, we measured changes in the number of reactive cysteine residues on tubulin after incubation with flubendazole. Treatment with flubendazole reduced the number of reactive cysteines by 5.2 plus or minus 2.6 compared with buffer control ( $P < .05$ ). In comparison, vinblastine decreased the number of reactive cysteines by 8.6 plus or minus 2.5 ( $P < .01$ ). Thus, these results suggest that flubendazole interacts with tubulin to alter its structure (Figure 3A).

Drugs that alter microtubules can either promote or inhibit tubulin polymerization.<sup>28</sup> Therefore, we evaluated the effects of flubendazole on tubulin polymerization. Flubendazole was incubated with purified bovine tubulin, and tubulin polymerization was recorded over time. As controls, bovine tubulin was incubated with colchicine, which is known to inhibit tubulin polymerization,<sup>29</sup> and taxol, which is known to promote tubulin polymerization.<sup>30</sup> In this assay, flubendazole inhibited tubulin polymerization (Figure 3B).

As flubendazole altered the structure and polymerization of tubulin, we compared its binding site with that of vinblastine, a member of the Vinca alkaloid family of microtubule inhibitors used for the treatment of leukemia and myeloma.<sup>31,32</sup> Purified bovine

tubulin was incubated with flubendazole or vinblastine followed by the addition of colchicine. The interaction of colchicine with tubulin was then assayed by measuring the fluorescence of colchicine bound to tubulin.<sup>33</sup> The addition of flubendazole decreased colchicine fluorescence, but the addition of vinblastine had no effect (Figure 3C), indicating that flubendazole, but not vinblastine, blocks colchicine from binding tubulin. Thus, flubendazole interacts with tubulin through a mechanism distinct from vinblastine.

Because flubendazole altered tubulin structure and function in cell-free assays, we evaluated the effects of flubendazole on microtubule formation in intact cells. PPC-1 prostate cancer cells were treated with flubendazole (1 μM) or vehicle control for 24 hours and then stained with antitubulin and 4,6-diamidino-2-phenylindole (DAPI). Microtubule architecture was visualized by confocal microscopy (Figure 3D). PPC-1 cells treated with vehicle control exhibited an organized network of elongated microtubules. In contrast, cells treated with flubendazole were rounded with contracted and disorganized microtubules. Thus, flubendazole disrupts the microtubule architecture in intact cells.

Microtubules mediate cell migration,<sup>34</sup> so we investigated the effects of flubendazole on cell migration with a wound healing assay. HeLa cells were seeded in 4-well chambers; and after adhering overnight, the cell monolayer was scratched to create a wound. Cells were treated with flubendazole or buffer control, and migration of cells to heal the wound was measured overtime. Treatment with flubendazole impaired cell migration and delayed wound healing (Figure 3E). Of note, at the concentrations and times tested in these assays, the flubendazole-treated cells were more than 89% viable as measured by MTS assay.

### Flubendazole arrests cells in cell cycle and induces mitotic catastrophe

Inhibition of tubulin polymerization can inhibit cell-cycle progression and induce mitotic catastrophe,<sup>35</sup> so we assessed the effects of flubendazole on the cell cycle by flow cytometry and on chromosomal segregation by enumerating the number of multinucleated cells in OCI-AML2 and PPC-1 cells. Flubendazole arrested cells in the G<sub>2</sub> phase of the cell cycle (Figure 4A-B) and increased the number of multinucleated cells (Figure 4C). Thus, flubendazole produces cell-cycle arrest and mitotic catastrophe, consistent with its effects as a microtubule inhibitor.

### Inhibition of microtubules is functionally important for flubendazole's cytotoxicity

Next, we determined whether inhibition of microtubule formation was functionally important for flubendazole's cytotoxicity. KB-4.0-HTI cells have a single nucleotide change in α-tubulin that renders it resistant to microtubule inhibitors.<sup>36</sup> Therefore, we treated KB-4.0-HTI and KB-3-1 wild-type controls with increasing concentrations of flubendazole and colchicine. Consistent with flubendazole's effects on tubulin, KB-4.0-HTI cells were more resistant to flubendazole with an IC<sub>50</sub> 7-fold higher than the nonmutated KB-3-1 wild-type cells (Table 1). Similarly, KB-4.0-HTI cells were also resistant to colchicine with an IC<sub>50</sub> 2.5-fold higher than the KB-3-1 control cells (Table 1), consistent with previous observations with this cell line.<sup>36</sup> Flubendazole was also tested in A549.EpoB40 cells, which are more sensitive to microtubule inhibitors because of a point mutation in β-tubulin at residue 292.<sup>37</sup> A549.EpoB40 cells were more sensitive to flubendazole with an

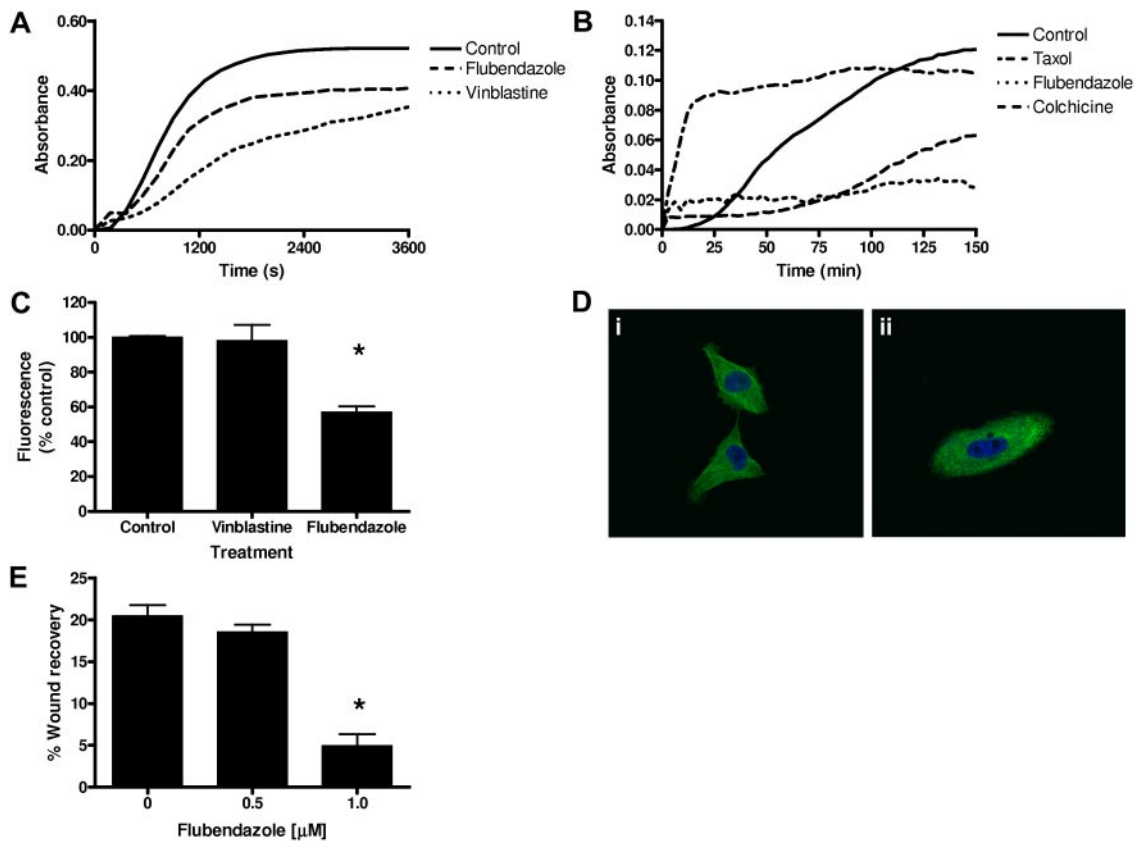


**Figure 3. Flubendazole inhibits tubulin structure, polymerization, and function.** (A) Flubendazole (100 $\mu$ M) and vinblastine (10 $\mu$ M) were incubated with bovine tubulin (1.5 $\mu$ M), and the conformational changes were monitored spectrophotometrically by measuring the decrease in the number of reactive cysteine residues at an absorbance of 412 nm as described in "Methods." A representative figure is shown. (B) Flubendazole (100 $\mu$ M), colchicine (6 $\mu$ M), and taxol (6 $\mu$ M) were incubated with bovine tubulin (1.8 mg/mL), and the effects on polymerization were monitored spectrophotometrically by measuring turbidity at 340 nm as described in "Methods." A representative figure is shown. (C) Tubulin (5 $\mu$ M) was incubated for 30 minutes with 100 $\mu$ M vinblastine, 100 $\mu$ M flubendazole, or buffer control. After incubation, colchicine (10 $\mu$ M) was added and incubated for 60 minutes. Fluorescence of the tubulin-colchicine complex was measured with excitation and emission wavelengths of 360 nm and 430 nm, respectively. Reduced fluorescence indicates binding at the colchicine site. \* $P < .01$  (analysis of variance, Bonferroni post hoc). A representative figure is shown. (D) PPC-1 cells were treated with vehicle control (i) or 1.0 $\mu$ M flubendazole (ii) for 24 hours and stained with DAPI and an anti- $\alpha$ -tubulin Alexa Fluor 488-nm antibody. Images were captured using an Olympus Fluorview confocal microscope at room temperature. Representative confocal micrographs (original magnification  $\times 40$ ) are shown. (E) HeLa cells were grown to confluence and a wound created on the cell monolayer using a 200- $\mu$ L pipette. Cells were treated with increasing concentrations of flubendazole and imaged every 2 hours for 8 hours. Wound healing was measured as described in the supplemental Methods. Representative data are shown and are presented as percentage wound recovery. \* $P < .05$  (analysis of variance, Bonferroni post hoc).

IC<sub>50</sub> 5-fold lower than the nonmutated A549 control cells (Table 1). Similarly, A549.EpoB40 cells were sensitive to colchicine with an IC<sub>50</sub> 1.5-fold lower than the A549 control cells (Table 1), consistent with previous observations with this cell line.<sup>37</sup> As further evidence that flubendazole's cytotoxicity was related to microtubule inhibition, the benzimidazoles thiabendazole and 1,3-benzidiazole that did not induce cell death in OCI-AML2 cells (Figure 1A) also did not inhibit microtubule formation in our cell-free polymerization assays (data not shown). Thus, taken together, flubendazole induces cell death through a mechanism that appears related to its inhibition of microtubule polymerization.

#### Overexpression of P-glycoprotein does not alter flubendazole's cytotoxicity

Overexpression of P-glycoprotein (Pgp, MDR1) renders cells resistant to Vinca alkaloid microtubule inhibitors.<sup>38</sup> Therefore, we tested the effects of Pgp overexpression on flubendazole's cytotoxicity. CEM-VBL cells overexpress Pgp,<sup>39</sup> which was confirmed with a rhodamine dye exclusion assay (data not shown). CEM wild-type and CEM-VBL cells were treated with increasing concentrations of flubendazole or vinblastine and cell viability was

measured by the MTS assay (Table 1). CEM-VBL cells remained fully sensitive to flubendazole compared with the wild-type controls. In contrast, CEM-VBL cells were resistant to vinblastine at concentrations greater than 5 $\mu$ M (Table 1). Therefore, because overexpression of Pgp does not abrogate the cytotoxicity of flubendazole, this drug is capable of overcoming some forms of resistance to Vinca alkaloids.

#### Flubendazole does not induce neuropathy

Neuropathy is a dose-limiting toxicity of Vinca alkaloid microtubule inhibitors, such as vincristine. Therefore, we tested the effects of flubendazole on neurologic function in mice. Mice (n = 10/group) were treated with 50, 100, or 200 mg/kg flubendazole or vehicle control intraperitoneally daily for 14 days, and sensory function was assessed with the tail-flick assay. No changes in tail-flick latency were observed at doses up to 200 mg/kg compared with controls, a dose 10-fold higher than the dose required for an antitumor effect (mean  $\pm$  SD tail-flick latency: control, 3.04  $\pm$  0.52 seconds vs 200 mg/kg flubendazole, 2.91  $\pm$  0.50 seconds,  $P = .58$  by Student *t* test). However,

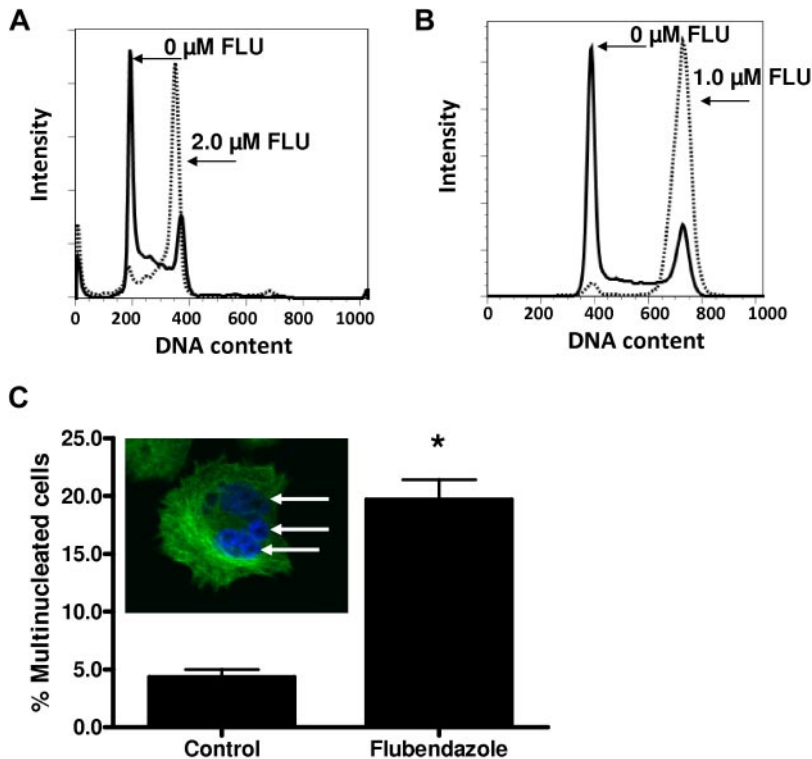


**Figure 4. Flubendazole induces cell-cycle arrest and mitotic catastrophe.** OCI-AML2 cells (A) or PPC-1 cells (B) were incubated with flubendazole or buffer control for 24 hours. Cells were then stained with PI, and the DNA content was measured by flow cytometry. A representative figure is shown. (C) PPC-1 cells were treated as in panel B and stained with anti- $\alpha$ -tubulin antibody and DAPI, as described in the supplemental Methods. Cells were imaged by confocal microscopy, and the number of multinucleated cells was enumerated. Data are the mean  $\pm$  SD percentage of multinucleated cells from a representative experiment. \* $P < .001$  (unpaired  $t$  test). (Inset) A representative multinucleated cell.

doses of 200 mg/kg resulted in 5% decrease in body weight compared with vehicle controls ( $P = .03$ , Student  $t$  test).

#### Flubendazole synergizes with vinblastine and enhances vinblastine and vincristine activity in vivo

Flubendazole interacts with tubulin through a mechanism distinct from vinblastine. Therefore, we evaluated the cytotoxicity of flubendazole and vinblastine in combination. OCI-AML2 cells were treated with increasing concentrations of flubendazole and vinblastine; and 72 hours after incubation, cell growth and viability were measured by the MTS assay. Combinations were assessed based on CI values where CI values less than 1, equal to 1, or more than 1 are considered synergistic, additive, or antagonistic, respectively.<sup>26,40</sup> The combination of flubendazole and vinblastine synergistically induced cell death with CI values of 0.09, 0.017, 0.003, and 0.001 at the 50% effective concentration ( $EC_{50}$ ),  $EC_{25}$ ,  $EC_{10}$ , and  $EC_5$ , respectively (Figure 5A). In contrast, cell death produced by the combination of flubendazole and colchicine was closer to additive with CI values of 0.54, 0.70, 0.90, and 1.07 at  $EC_{50}$ ,  $EC_{25}$ ,

$EC_{10}$ , and  $EC_5$ , respectively (Figure 5B). Combinations of flubendazole and cytarabine or daunorubicin were also closer to additive (Figure 5C-D).

Given the synergy of flubendazole and vinblastine in cell culture, we evaluated the combination of flubendazole and vinblastine and vincristine in vivo. OCI-AML2 cells were injected subcutaneously into SCID mice and treated intraperitoneally with flubendazole (15 mg/kg), vinblastine (0.3 mg/kg), or vincristine (0.25 mg/kg), or the combination of the 2 agents. The combination of flubendazole and vinblastine decreased tumor weight greater than either agent alone ( $P < .01$ ; Figure 6A). Similarly, the combination of flubendazole and vincristine decreased tumor weight and volume greater than either agent alone ( $P < .001$ ; Figure 6B). Moreover, there were no observed behavioral changes, weight loss, or gross organ toxicity from either combination treatment (supplemental Figure 2). Of note, however, despite dramatic reductions in tumor growth even with established tumors, neither flubendazole, nor vincristine, nor the combination of these agents caused tumor regression in this mouse model (Figure 6C). Thus, flubendazole synergizes with vinblastine and vincristine and could be used in combination with these Vinca alkaloids to achieve a greater antitumor effect.

**Table 1. Flubendazole reduces cell growth and viability in malignant cells**

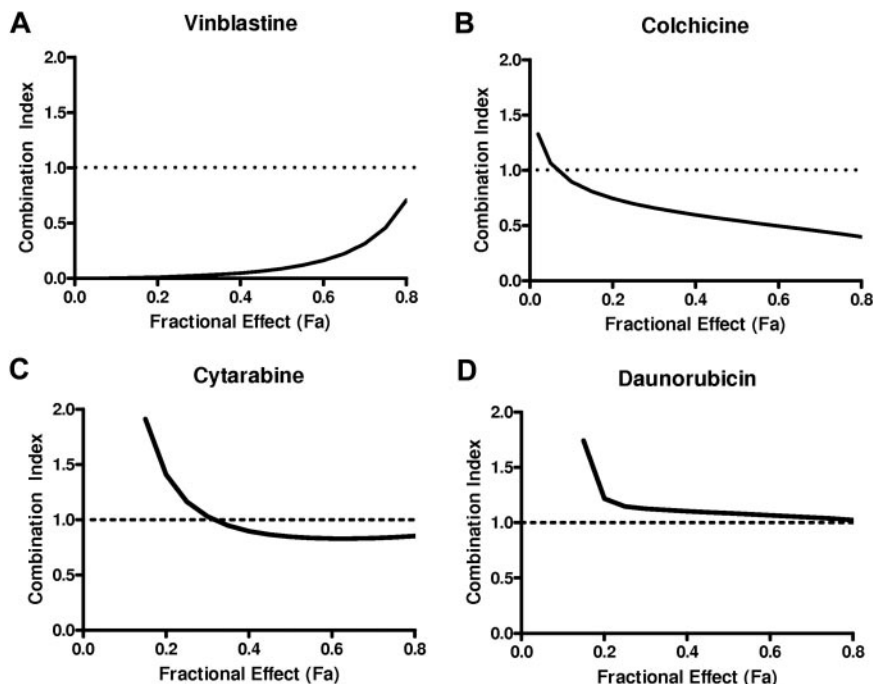
Cell line	Flubendazole, $\mu$ M	Colchicine, nM	Vinblastine, $\mu$ M
KB-3-1	1.9 $\pm$ 1.1	14.9 $\pm$ 4.5	
KB-4.0-HTI	12.5 $\pm$ 1.8	41.6 $\pm$ 5.5	
A549	4.1 $\pm$ 1.3	0.09 $\pm$ 0.01	
A549.EpoB40	0.8 $\pm$ 0.2	0.06 $\pm$ 0.01	
CEM	1.9 $\pm$ 0.9		0.14 $\pm$ 0.01
CEM-VBL	2.7 $\pm$ 1.2		> 5.0

KB-4.0-HTI cells with an  $\alpha$ -tubulin mutation and KB-3-1 wild-type controls, A549.EpoB40 cells with a  $\beta$ -tubulin mutation and the A549 wild-type controls, and CEM VBL cells overexpressing P-glycoprotein and CEM wild-type controls were treated with increasing concentrations of flubendazole for 72 hours. Data represent  $IC_{50}$  values, as measured by the MTS assay.

## Discussion

Through screens of libraries of on-patent and off-patent drugs, we identified flubendazole as having previously unrecognized antileukemia and antimyeloma activity. At pharmacologically achievable concentrations, flubendazole induced cell death in malignant cells and delayed tumor growth in vivo. Mechanistically, flubendazole altered microtubule structure and inhibited tubulin polymerization by interacting with a site on tubulin similar to colchicine and distinct from vinblastine.

**Figure 5. Flubendazole synergizes with vinblastine.** The effects of increasing concentrations of flubendazole in combination with vinblastine (A), colchicine (B), cytarabine (C), or daunorubicin (D) on the viability of OCI-AML2 cells. Cell viability was measured by the MTS assay after 72 hours of incubation. Data were analyzed with Calcsyn software as described in "Methods." CI versus fractional effect (Fa) plot showing the effect of the combination of flubendazole and vinblastine, colchicine, cytarabine, or daunorubicin. CI < 1 indicates synergism. One of 2 representative isobologram experiments performed in triplicate is shown.



As part of its development as an antihelminthic, flubendazole has been studied extensively in animals and humans, where it has displayed favorable toxicology profiles. For example, in rats, mice, and guinea pigs, the LD<sub>50</sub> is more than 5000 mg/kg and more than 400 mg/kg after oral and intraperitoneal administration, respectively.<sup>10</sup> No toxicity was noted in rats that received up to 150 mg/kg/d for 3 months, whereas chickens receiving up to 180 mg/kg flubendazole daily for 7 days developed anemia and reduction of red cells in the spleen.<sup>10</sup> In humans, doses of 40 to 50 mg/kg/d for 10 days have been administered for the treatment of neurocysticercosis, and no toxicity from the drug was reported.<sup>9</sup> Likewise, patients received up to 50 mg/kg/d of flubendazole for up to 24 months for the treatment of alveolar echinococcosis without adverse effect.<sup>8</sup>

The pharmacokinetics of flubendazole are also well characterized. For example, in sheep, the estimated half-life for flubendazole

after oral administration is 6.5 hours and the main metabolic pathways are carbamate hydrolysis and ketone reduction.<sup>10</sup> After intravenous administration, an AUC of 6.53 μg/hour per milliliter is achieved over 36 hours after a single intravenous dose of 5 mg/kg. However, only 18% of flubendazole is absorbed, so after a single oral dose of 5 mg/kg of the AUC over 36 hours was 1.17 μg/hour per milliliter.<sup>41</sup> The oral bioavailability of flubendazole is better, however, in mice. After oral administration of 5 mg/kg flubendazole to mice, an AUC of 2.17 μg/hour per milliliter and a C<sub>max</sub> of 1.12 μg/mL (3.6 μM) were achieved without toxicity.<sup>11</sup> Although the extent to which flubendazole is bound to proteins in the plasma is unclear, albendazole, a compound with similar absorption properties and structure as flubendazole,<sup>42</sup> has an estimated plasma protein binding of 70%. If the plasma protein binding was similar for flubendazole, then a C<sub>max</sub> of 1.12 μg/mL would equate to 0.34 μg/mL (1.1 μM) of free flubendazole. This

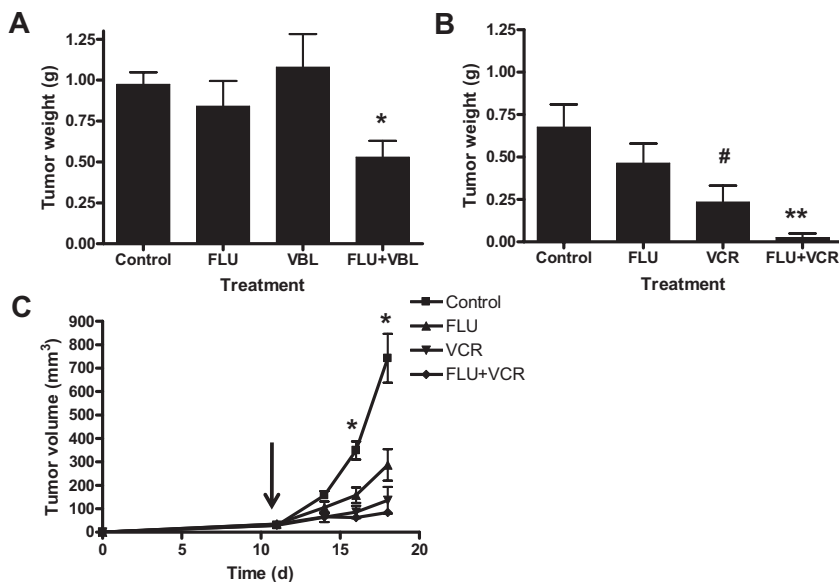


**Figure 6. Flubendazole enhances the activity of Vinca alkaloids in vivo.** Sublethally irradiated SCID mice were injected subcutaneously with OCI-AML2 cells (n = 40; 10 per group). After implantation, mice were treated with (A) 15 mg/kg flubendazole, 0.3 mg/kg vinblastine, a combination of flubendazole and vinblastine, or vehicle control; or (B) 20 mg/kg flubendazole, 0.25 mg/kg vincristine, a combination of flubendazole and vincristine, or vehicle control. After 16 (A) or 18 (B) days, mice were killed and tumors were excised, measured, and weighted. (C) Sublethally irradiated SCID mice were injected subcutaneously with OCI-AML2 cells (n = 40; 10 per group). Eleven days after injection, when tumors were established (eg, tumor volume = 32 mm<sup>3</sup>), mice were treated with 50 mg/kg flubendazole, 0.25 mg/kg vincristine (VCR), the combination of flubendazole and VCR, or vehicle control. Tumor volume was measured over time with calipers. Data are the mean ± SD tumor weight. A representative experiment is shown. #P < .05, \*P < .01, \*\*P < .001, compared with controls (unpaired t test).



value compares very favorably to our reported submicromolar IC<sub>50</sub> values for flubendazole's cytotoxicity in malignant cells.

It is unknown whether the current oral formulation of flubendazole would be suitable for the treatment of patients with malignancy as the oral bioavailability of the current formulation is low in humans.<sup>10</sup> However, because large doses can be safely administered and are sufficient to treat systemic worm infections, the current formulation might be suitable for the treatment of hematologic malignancies. Alternatively, an intravenous formulation or an oral formulation with improved bioavailability could be developed but might require additional pharmacokinetic and/or toxicology testing before clinical trial.

Our clonogenic assays did not demonstrate a difference between the cytotoxicity of flubendazole for primary AML and normal hematopoietic cells, and this finding raises concerns regarding the potential therapeutic window of flubendazole. However, it is important to note that results of colony formation assays do not always predict clinical toxicity. For example, cytarabine and m-AMSA (N-[4-(9-acridinylamino)-3-methoxyphenyl]-methanesulfonamide), which are routinely used in the treatment of AML, show little or no selectivity for malignant cells over normal cells in colony formation assays.<sup>43,44</sup> Likewise, the microtubule inhibitor vincristine does not show preferential cytotoxicity to malignant cells over normal hematopoietic cells in vitro.<sup>45</sup> Moreover, we observed that oral flubendazole delayed tumor growth in mouse models of leukemia and myeloma without toxicity. Finally, toxicology studies with flubendazole conducted in mice and sheep did not report hematologic toxicity.<sup>10</sup> Nonetheless, the lack of difference between primary AML and normal hematopoietic cells in the clonogenic assay raises concerns about the potential hematologic toxicity, and its safety will have to be carefully evaluated in phase I clinical trials.

Vinca alkaloids are currently used in the treatment of myeloma but are not part of standard induction chemotherapy for patients with AML. It is interesting to note, however, that induction chemotherapy for AML in the 1970s used vincristine in combination with cyclophosphamide and cytarabine or cyclophosphamide and daunorubicin.<sup>46,47</sup> In the 1980s, this regimen was replaced with daunorubicin and cytarabine, and vincristine was dropped from the protocol. However, it has never been determined whether addition of vincristine to daunorubicin and cytarabine would provide any additional benefit. These early studies, nonetheless, demonstrate the efficacy of tubulin inhibitors in AML and suggest that they could be beneficial in some patients, possibly in the setting of relapsed disease.

In support of the evaluation of flubendazole for the treatment of patients with refractory hematologic malignancies, a phase I clinical trial of the related benzimidazole, albendazole was recently conducted in patients with advanced solid tumors.<sup>48</sup> In 2 of 7 patients, albendazole reduced levels of the tumor markers  $\alpha$ -fetoprotein and carcinoembryonic antigen. However, albendazole caused severe neutropenia in 3 of these patients, and the development of albendazole as an antitumor agent has not been pursued to date.

In our study, flubendazole inhibited tubulin polymerization and function, which were functionally important for its cytotoxicity. Microtubules are cytoskeleton components that are required for cell division, cellular transport, and in the maintenance of cellular integrity.<sup>28</sup> Microtubules are composed of  $\alpha$ - and  $\beta$ -tubulin heterodimers that assemble into linear protofilaments and polymerize into hollow, cylindrical structures.<sup>31</sup> The gain or loss of tubulin heterodimers leads to elongation or shortening of the microtubules.<sup>49</sup> Drugs that alter the polymerization of microtubules are well-validated therapeutic agents for the treatment of malignancies.

For example, Vinca alkaloids inhibit microtubule polymerization by binding to  $\beta$ -tubulin near the guanosine triphosphate-binding site.<sup>31</sup> In contrast, colchicine inhibits polymerization by binding the interface of the  $\alpha/\beta$ -tubulin heterodimer and taxol promotes tubulin polymerization by binding in the lumen of the polymer.<sup>31</sup> In our study, we demonstrated that flubendazole interacts with tubulin at a site similar to that of colchicine and distinct from Vinca alkaloids. A similar interaction with tubulin has been reported for the benzimidazole mebendazole.<sup>50</sup> However, the benzimidazole benmethyl has been reported to inhibit tubulin polymerization by interacting at a site distinct from both the colchicine site and the Vinca domain.<sup>13</sup> Thus, the mechanism by which benzimidazoles inhibit tubulin formation appears to vary among family members.

As flubendazole and Vinca alkaloids inhibited tubulin through distinct mechanisms, we evaluated the combination of these drugs. Flubendazole synergized with the Vinca alkaloids vinblastine and vincristine in vitro and in vivo. Therefore, these drugs could be used in combination to enhance the efficacy of standard therapy for these diseases or potentially reduce their toxicity.

Finally, as flubendazole inhibits tubulin function through a mechanism distinct from Vinca alkaloids, flubendazole could be useful in overcoming some forms of resistance to Vinca alkaloids. For example, as overexpression of Pgp does not render cells resistant to flubendazole, it could also overcome this specific mechanism of resistance to Vinca alkaloids.

In conclusion, flubendazole is a novel microtubule inhibitor that acts through a mechanism distinct from Vinca alkaloids. Given its prior safety record in humans and animals coupled with its preclinical efficacy in hematologic malignancies demonstrated here, flubendazole could be repurposed for evaluation in these diseases.

## Acknowledgments

The authors thank Drs Frank Loganzo (Oncology Research, Wyeth Research, Pearl River, NY), John Dick (University Health Network, Toronto, ON), and Susan Band Horwitz and Chia-Ping Yang (Albert Einstein College of Medicine, Bronx, NY) for critical reagents.

This study was supported by the Terry Fox Foundation (research grants; A.D.S.), the Ministry of Research and Innovation and the Ministry of Long Term Health and Planning both in the Province of Ontario.

A.D.S. is a Leukemia & Lymphoma Society Scholar in Clinical Research.

## Authorship

Contribution: P.A.S. and A.D.S. designed and performed research, analyzed data, and wrote the paper; J.H., R.H., M.G., M.A.S., and R.B.Z. designed and performed research and analyzed data; X.W. and S.S. performed research and analyzed data; A.D., J.B., I.A., and C.D.S. performed research and analyzed data; N.F. and R.R. designed research; and all authors reviewed and edited the paper.

Conflict-of-interest disclosure: The authors declare no competing financial interests.

Correspondence: Aaron D. Schimmer, 610 University Ave, Rm 9-516, Toronto, ON, M5G 2M9; e-mail: aaron.schimmer@toronto.ca.

## References

- Vazquez-Martin A, Oliveras-Ferreros C, del Barco S, Martin-Castillo B, Menendez JA. The antidiabetic drug metformin: a pharmaceutical AMPK activator to overcome breast cancer resistance to HER2 inhibitors while decreasing risk of cardiomyopathy. *Ann Oncol*. 2009;20(3):592-595.
- Ben Sahra I, Laurent K, Loubat A, et al. The antidiabetic drug metformin exerts an antitumoral effect in vitro and in vivo through a decrease of cyclin D1 level. *Oncogene*. 2008;27(25):3576-3586.
- Li D, Yeung SC, Hassan MM, Konopleva M, Abbruzzese JL. Antidiabetic therapies affect risk of pancreatic cancer. *Gastroenterology*. 2009;137(2):482-488.
- Cazzaniga M, Bonanni B, Guerrieri-Gonzaga A, Decensi A. Is it time to test metformin in breast cancer clinical trials? *Cancer Epidemiol Biomarkers Prev*. 2009;18(3):701-705.
- Larkin M. Low-dose thalidomide seems to be effective in multiple myeloma. *Lancet*. 1999;354(9182):925.
- Richardson PG, Mitsiades CS, Munshi NC, Anderson KC. Can thalidomide improve outcome in patients with multiple myeloma? *Nat Clin Pract Oncol*. 2006;3(11):590-591.
- Feldmeier H, Bienze U, Dohring E, Dietrich M. Flubendazole versus mebendazole in intestinal helminthic infections. *Acta Trop*. 1982;39(2):185-189.
- Lassègue A, Estavoyer JM, Minazzi H, et al. Treatment of human alveolar echinococcosis with flubendazole: clinical, morphological and immunological study. *Gastroenterol Clin Biol*. 1984;8(4):314-320.
- Téllez-Girón E, Ramos MC, Dufour L, et al. Treatment of neurocysticercosis with flubendazole. *Am J Trop Med Hyg*. 1984;33(4):627-631.
- Fuchs R. *Flubendazole*. Vol 31. Geneva, Switzerland: World Health Organization; 1993.
- Ceballos L, Elissondo M, Bruni SS, Denegri G, Alvarez L, Lanusse C. Flubendazole in cystic echinococcosis therapy: pharmacoparasitological evaluation in mice. *Parasitol Int*. 2009;58(4):354-358.
- Doudican N, Rodriguez A, Osman I, Orlow SJ. Mebendazole induces apoptosis via Bcl-2 inactivation in chemoresistant melanoma cells. *Mol Cancer Res*. 2008;6(8):1308-1315.
- Gupta K, Bishop J, Peck A, Brown J, Wilson L, Panda D. Antimitotic antifungal compound benomyl inhibits brain microtubule polymerization and dynamics and cancer cell proliferation at mitosis, by binding to a novel site in tubulin. *Biochemistry*. 2004;43(21):6645-6655.
- Cumino AC, Elissondo MC, Denegri GM. Flubendazole interferes with a wide spectrum of cell homeostatic mechanisms in *Echinococcus granulosus* protoscoleces. *Parasitol Int*. 2009;58(3):270-277.
- Jasra N, Sanyal SN, Khera S. Effect of thiazolidazole and fenbendazole on glucose uptake and carbohydrate metabolism in *Trichuris globulosa*. *Vet Parasitol*. 1990;35(3):201-209.
- Lacey E, Watson TR. Activity of benzimidazole carbamates against L1210 mouse leukaemia cells: correlation with in vitro tubulin polymerization assay. *Biochem Pharmacol*. 1985;34(19):3603-3605.
- Xu GW, Ali M, Wood TE, et al. The ubiquitin-activating enzyme E1 as a therapeutic target for the treatment of leukemia and multiple myeloma. *Blood*. 2010;115(11):2251-2259.
- Mawji IA, Simpson CD, Hurren R, et al. Critical role for Fas-associated death domain-like interleukin-1-converting enzyme-like inhibitory protein in anoikis resistance and distant tumor formation. *J Natl Cancer Inst*. 2007;99(10):811-822.
- Santra M, Santra S, Roberts C, Zhang RL, Chopp M. Doublecortin induces mitotic microtubule catastrophe and inhibits glioma cell invasion. *J Neurochem*. 2009;108(1):231-245.
- Wood TE, Dalili S, Simpson CD, et al. A novel inhibitor of glucose uptake sensitizes cells to FAS-induced cell death. *Mol Cancer Ther*. 2008;7(11):3546-3555.
- Beyer CF, Zhang N, Hernandez R, et al. TTI-237: a novel microtubule-active compound with in vivo antitumor activity. *Cancer Res*. 2008;68(7):2292-2300.
- Roychowdhury M, Sarkar N, Manna T, et al. Sulfhydryls of tubulin: a probe to detect conformational changes of tubulin. *Eur J Biochem*. 2000;267(12):3469-3476.
- Beheshti Zavareh R, Lau KS, Hurren R, et al. Inhibition of the sodium/potassium ATPase impairs N-glycan expression and function. *Cancer Res*. 2008;68(16):6688-6697.
- Mao X, Li X, Sprangers R, et al. Clioquinol inhibits the proteasome and displays preclinical activity in leukemia and myeloma. *Leukemia*. 2009;23(3):585-590.
- Grover VS, Sharma A, Singh M. Role of nitric oxide in diabetes-induced attenuation of antinociceptive effect of morphine in mice. *Eur J Pharmacol*. 2000;399(2):161-164.
- Chou TC, Talalay P. Quantitative analysis of dose-effect relationships: the combined effects of multiple drugs or enzyme inhibitors. *Adv Enzyme Regul*. 1984;22:27-55.
- Sharmeen S, Skrtic M, Sukhai M, et al. Activation of chloride channels by the anti-parasitic agent ivermectin induces membrane hyperpolarization and cell death in leukemia cells. *American Society of Hematology*, New Orleans, LA, December 7, 2009.
- Jordan MA, Wilson L. Microtubules as a target for anticancer drugs. *Nat Rev Cancer*. 2004;4(4):253-265.
- Sternlicht H, Ringel I. Colchicine inhibition of microtubule assembly via copolymer formation. *J Biol Chem*. 1979;254(20):10540-10550.
- Manfredi JJ, Parness J, Horwitz SB. Taxol binds to cellular microtubules. *J Cell Biol*. 1982;94(3):688-696.
- Risinger AL, Giles FJ, Mooberry SL. Microtubule dynamics as a target in oncology. *Cancer Treat Rev*. 2009;35(3):255-261.
- Zelnak AB. Clinical pharmacology and use of microtubule-targeting agents in cancer therapy. *Methods Mol Med*. 2007;137:209-234.
- Bhattacharyya B, Wolff J. Promotion of fluorescence upon binding of colchicine to tubulin. *Proc Natl Acad Sci U S A*. 1974;71(7):2627-2631.
- Gao J, Huo L, Sun X, et al. The tumor suppressor CYLD regulates microtubule dynamics and plays a role in cell migration. *J Biol Chem*. 2008;283(14):8802-8809.
- Jordan MA, Kamath K, Manna T, et al. The primary antimitotic mechanism of action of the synthetic halichondrin E7389 is suppression of microtubule growth. *Mol Cancer Ther*. 2005;4(7):1086-1095.
- Loganzo F, Hari M, Annable T, et al. Cells resistant to HTI-286 do not overexpress P-glycoprotein but have reduced drug accumulation and a point mutation in alpha-tubulin. *Mol Cancer Ther*. 2004;3(10):1319-1327.
- He L, Yang CP, Horwitz SB. Mutations in beta-tubulin map to domains involved in regulation of microtubule stability in epothilone-resistant cell lines. *Mol Cancer Ther*. 2001;1(1):3-10.
- Dumontet C, Sikic BI. Mechanisms of action of and resistance to antitubulin agents: microtubule dynamics, drug transport, and cell death. *J Clin Oncol*. 1999;17(3):1061-1070.
- Huang TH, Bebawy M, Tran VH, Roufogalis BD. Specific reversal of multidrug resistance to colchicine in CEM/VLB(100) cells by *Gynostemma pentaphyllum* extract. *Phytomedicine*. 2007;14(12):830-839.
- Chou TC. Preclinical versus clinical drug combination studies. *Leuk Lymphoma*. 2008;49(11):2059-2080.
- Moreno L, Alvarez L, Mottier L, Virkel G, Bruni SS, Lanusse C. Integrated pharmacological assessment of flubendazole potential for use in sheep: disposition kinetics, liver metabolism and parasite diffusion ability. *J Vet Pharmacol Ther*. 2004;27(5):299-308.
- Castro N, Marquez-Caraveo C, Brundage RC, et al. Population pharmacokinetics of albendazole in patients with neurocysticercosis. *Int J Clin Pharmacol Ther*. 2009;47(11):679-685.
- Singer CR, Linch DC. Comparison of the sensitivity of normal and leukemic myeloid progenitors to in-vitro incubation with cytotoxic drugs: a study of pharmacological purging. *Leuk Res*. 1987;11(11):953-959.
- Spiro TE, Socquet M, Delforge A, Stryckmans P. Chemotherapeutic sensitivity of normal and leukemic hematopoietic progenitor cells to N-[4-(9-acridinylamino)-3-methoxyphenyl]-methanesulfonamide, a new anticancer agent. *J Natl Cancer Inst*. 1981;66(4):615-618.
- Cardinali G, Cardinali G, Enein MA. Studies on the antimitotic activity of leurocristine (Vincristine). *Blood*. 1963;21(1):102-110.
- Coltman CA Jr, Bodey GP, Hewlett JS, et al. Chemotherapy of acute leukemia: a comparison of vincristine, cytarabine, and prednisone alone and in combination with cyclophosphamide or daunorubicin. *Arch Intern Med*. 1978;138(9):1342-1348.
- Curtis JE, Cowan DH, Bergsagel DE, Hasselback R, McCulloch EA. Acute leukemia in adults: assessment of remission induction with combination chemotherapy by clinical and cell-culture criteria. *Can Med Assoc J*. 1975;113(4):289-294.
- Morris DL, Jourdan JL, Pourgholami MH. Pilot study of albendazole in patients with advanced malignancy: effect on serum tumor markers/high incidence of neutropenia. *Oncology*. 2001;61(1):42-46.
- Westermann S, Weber K. Post-translational modifications regulate microtubule function. *Nat Rev Mol Cell Biol*. 2003;4(12):938-947.
- Ireland CM, Gull K, Gutteridge WE, Pogson CI. The interaction of benzimidazole carbamates with mammalian microtubule protein. *Biochem Pharmacol*. 1979;28(17):2680-2682.